Zero-Point Correction Method for Nanoindentation Tests to Accurately Quantify Hardness and Indentation Size Effect

J. Marteau, Salima Bouvier, Maxence Bigerelle

Zero-Point Correction Method for Nanoindentation Tests to Accurately Quantify Hardness and Indentation Size Effect

J. Marteau*, P.-E. Mazeran*, S. Bouvier* and M. Bigerelle†

*Laboratoire Roberval, UMR 7337, Université de Technologie de Compiègne, Centre de Recherches de Royallieu, BP 20529, 60205 Compiègne Cedex, France

†Laboratoire Thermique, Energétique, Mise en forme, Production EA 4542, Université de Valenciennes et du Hainaut Cambrésis, Le Mont Houy, 59313 Valenciennes, France

ABSTRACT: An original treatment method is proposed to accurately determine by nanoindentation, the macrohardness and the indentation size effect (ISE). This method is applied to stainless steel specimens having different rough surfaces. It uses load versus indentation depth curves and is based on two main original features. The first one concerns the correction of the zero point (i.e. depth equals to 0) to minimise the scattering between experimental curves. The latter are all described by usual hardness equations and are shifted by minimising the distance from a leading curve chosen in a random way among the experimental curves. The second feature is the simultaneous treatment of all the nanoindentation curves to compute the macrohardness and evaluate the ISE. The standard deviation for the estimated macrohardness is small, which indicates the robustness of the approach. It is shown that using a single nanoindentation curve can alter macrohardness estimation because of a bad consideration of the ISE. To prevent this misinterpretation, the curves should be treated simultaneously instead of averaging results of separately treated curves. A correlation is identified between the standard deviations of both surface roughness and correction of zero point, which highlights the effect of surface roughness on the scattering of the indentation curves.

KEY WORDS: *hardness, indentation size effect, nanoindentation, roughness, zero point*

Introduction

Instrumented indentation is part of the more used tools for the characterisation of thin films [1] and material surface [2]. It can be employed for the identification of elastic properties [3], plastic properties [4] or viscoelastic properties [5]. However, the calculated material parameters often show important variations caused by a lack of rigorous data analysis. One of the most important issues is the first contact detection [6]. Classical nanoindenters are programmed to monitor a certain parameter (e.g. harmonic constant stiffness) whose threshold is set by the user. Once the limit is reached, the indentation depth is set to zero. The zero point is thus considerably influenced by the material rigidity, surface forces or contamination, the choice of the parameter threshold and finally the specimen roughness.

To try to compensate the uncertain position of the first contact, several methods have been developed. One method is based on the monitoring of the force value [7]. Once, a pre-set force is reached by the device, the indentation depth is set to zero. Then, the load versus indentation depth curve is fitted to the experimental data and then extrapolated back to zero force. It gives an initial penetration depth which is subtracted from the experimental data. The main drawback of this method is that it requires some knowledge on the material properties to correctly set the initial force value. Other authors have chosen to fit the first nanometres (about 30 nm) of the loading data with a power-law equation before extrapolating back to zero indentation depth [8]. Similar methods are based on the use of second-order polynomials [9]. Finally, some methods distinguish themselves from the previous ones by modifying the definition of the zero point [10]. Instead of searching for the initiation of contact, they use a point that is consistent with the Hertz's theory. They perform a regression analysis on the initial elastic part of the loading curve and fit it with a relationship established using Hertz's theory. However, this new definition can only be applied with spherical indenters. The previous methods are designed to correct the zero-point position through the calculation or the extrapolation of experimental data. Most of them focus their research on the first few nanometres or on a position near zero force. But, the experimental noise has a particularly important effect at the nanometre scale.

In this work, we propose to correct the zero-point errors using the evolution predicted by macroscopic behaviour laws. An original approach for the data analysis of nanoindentation curves is proposed. The latter is based on the definition of a deviation between the experimental data and the evolution depicted by usual hardness equations. The effectiveness of our method is also reinforced by the consideration of the indentation size effect (ISE) during the treatment of the curves. Both features aim at accurately determining the material macrohardness and quantifying the size effects. Finally, we ensure the result accuracy by having a good statistical representativeness of the specimen properties thanks to the simultaneous use of several loading curves. In this study, one hundred loading curves are studied as a whole. This method is applied to four specimens of 316L stainless steel having mirror-like surface (paper grit 4000) to rough surface (paper grit 80) to determine the evolution of the macrohardness and the ISE with roughness. The different magnitudes of abrasive surface are then used to quantify the effect of roughness on the first- contact detection.

The second part of this study describes the experimentation and the pre-treatment realised on the experimental

data. Then, the data treatment method is presented with the theory used to build it. The results given by this method are presented and discussed before summarising the main findings of this study.

Experimental Details

Material and mechanical polishing

The samples are cut from a 30-mm-diameter bar of 316L stainless steel into 20-mm thick discs. This steel is composed of a single austenitic phase. The chemical composition is indicated in Table 1.

The stainless steel specimens are abraded using an automatic grinding machine with off-centred rotating movements. First, the four specimens are polished up to paper grit 4000 to obtain mirror-like surfaces. This step enables to obtain similar initial mechanical states. Then, different magnitudes of deterioration are achieved by polishing the specimens using either paper grit 80 or 220 or 800 under identical conditions of load and pressure (150′N, 3 min) with water lubrication. In the following sections, for conciseness, the four specimens will be designated using the paper grit number used to polish them.

Table 1: Chemical composition of 316L stainless steel

Composition	C	Si	Mn	Ni	Cr	Mo	N	S	P	Cu	Fe
% Weight	0.008	0.27	1.62	14.58	17.58	2.8	0.06	0.001	0.014	0.07	–

Roughness measurements

The abraded specimen topography is measured using a tactile profilometer 3D TENSOR™ P10. Examples of topography are given in Figure 1. Roughness is recorded with a stylus having a 2-μm tip under a load equal to 5.10^{-5}′N, with a nanometre order of magnitude for the vertical resolution. A series of preliminarytridimensional measurements are realised on 4×4 mm areas to evaluate the specimen topography. As these first results show that a hypothesis of isotropy can be supported, the specimen topography is more accurately analysed using two-dimensional profiles recorded on a 5 mm length with a higher sampling frequency. For each specimen, 30 two-dimen-

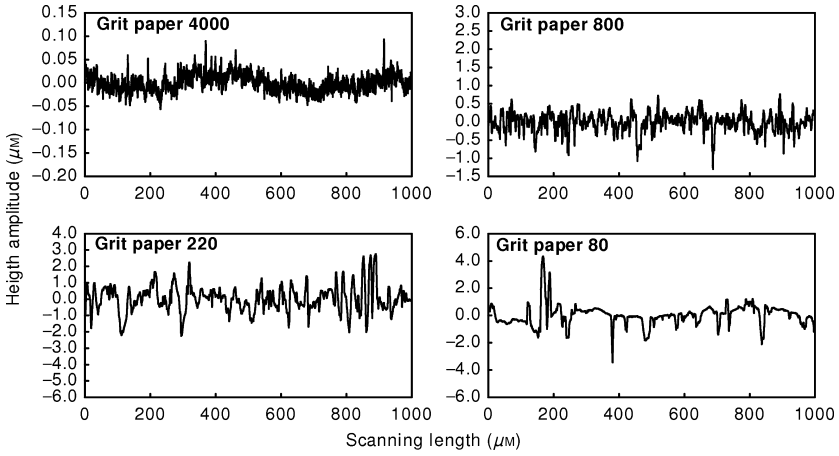

Figure 1: Profiles of the specimens polished with paper grit 80, 220, 800 and 4000

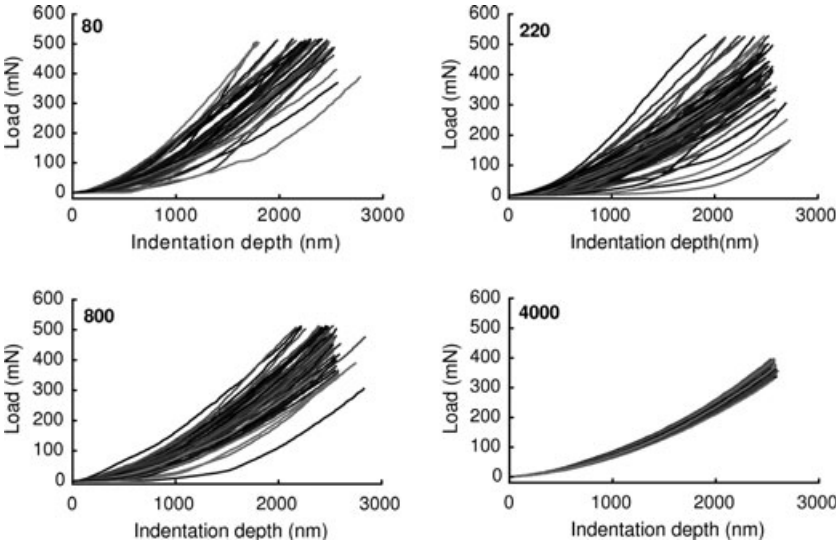

Figure 2: Loading part of the load versus indentation depth curves for the stainless steel specimens polished with paper grit 80, 220, 800 and 4000

sional profiles of 25 000 points are randomly recorded on the surface with a speed equal to 200 μm s^{-1}.

Nanoindentation tests

The nanoindentation tests are realised at ambient temperature using a Nano Indenter XP® equipped with a Berkovich tip. Using the continuous stiffness method (CSM) with a constant strain rate equal to 0.05 s^{-1}, a maximum penetration depth of 2500 nm is achieved. The nanoindentation tests give three parameters used to calculate local mechanical characteristics: the contact stiffness (S), the load (P) and the indentation depth (h). One hundred indents are made into each stainless steel specimen. Figure 2 shows the loading curves obtained for the four specimens.

Pre-Treatment of the Data

Pre-treatment of the nanoindentation loading curves

The calculation of the mechanical parameters (see 'Proposition of a new treatment method' section) are based on the use of the loading part of the nanoindentation curves. To avoid statistical artefacts, three pre-treatments are carried out.

First, we extracted the loading curve from the experimental measurements by limiting the data to a threshold equal to 0.85 P_{max} where P_{max} is the maximum experimental load. This truncation helps having a same final load for all the curves to avoid any statistical artefact when treating the data.

A second pre-treatment consists in converting the indentation depth h into an independent and identically distributed variable to avoid any bias during later nonlinear regression. Thus, each 20 nm, the loading data are averaged.

A last pre-treatment consists in converting the indentation depth h into the contact depth h_c defined by Oliver and Pharr [11] as follows:

$$h_c = h - \varepsilon P/S, \tag{1}$$

where ε is equal to 0.75 for a Berkovich indenter and S stands for the contact stiffness. From the section dealing with the 'Original statistical treatment', only the contact depth will be used.

Multiscale pre-treatment of two-dimensional experimental profiles

One of the main issues in roughness parameter analysis is the determination of the evaluation length, and the reference line (i.e. the fitting polynomial degree) from which the roughness parameters are calculated [12]. The correct assessment of the evaluation length requires the splitting of each experimental profile into equal parts. Then, to remove the variations that are higher than the evaluation length, each part of the profile is rectified using a three degree polynomial and the least square adjustment method. The removing of local variations is performed by calculating regression parameters on a given window. C^0 continuity is imposed on adjacent lines crossing neighbouring windows. It allows rectifying the profile by subtracting the calculated B-spline curve. Basically, this treatment is similar to a high-pass filtering revealing the microroughness.

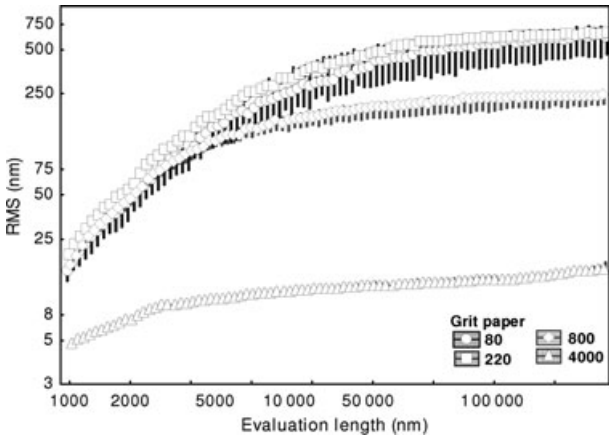

Figure 3: Evolution of the root-mean-square (RMS) roughness versus the evaluation length

Using the rectified profiles, the root-mean-square (RMS) roughness called R_q in ISO-4287 [13] is calculated on all the subparts having a fixed evaluation length.

This value is calculated on several evaluation lengths for each specimen and then averaged. Figure 3 depicts the average RMS roughness obtained as function of the evaluation length. For the specimens polished with paper grit 80, 220 and 800, the roughness increases with the evaluation length before stabilising. The curve corresponding to the specimen abraded with paper grit 4000 is different from the others because of an apparent waviness [14–16].

Theory and Method

Theory

The method presented in this study is based on Kick's law [17], which is a particular case of Meyer's law [18] where Meyer's index is equal to 2.

For geometrically similar indenters, the nanoindentation loading curve is usually expressed using a parabolic relationship known as Kick's law:

$$P = Ch^2, \tag{2}$$

where P is the load, h is the indentation depth and C is a constant which only depends on the indenter geometry for an ideal indenter.

It is assumed that there is an error on the zero-point detection which entails a gap Δh between the positions of the experimental curves. Hence, the penetration depth h in Equation 2 should be corrected to take into account Δh, leading to:

$$P = C(h + \Delta h)^2 = Ch^2 + 2Ch\Delta h + C\Delta h^2, \tag{3}$$

Δh is introduced to 'correct' the error in the measurement of the indentation depth h. The value of the deviation, Δh is low compared with the indentation depth h, hence the term $C\Delta h^2$ can be neglected:

$$P = Ch^2 + 2Ch\Delta h. \tag{4}$$

The obtained formula is similar to Bernhardt's law [19], an extension of Kick's law that allows to take into account

the hardness variation with the indentation depth, expressed by:

$$P = a_1 h^2 + a_2 h, \tag{5}$$

where a_1 and a_2 are constants. This formula is equivalent to the one of the proportional specimen resistance (PRS) proposed by Li and Bradt [20]:

$$P = b_1 d^2 + b_2 d, \tag{6}$$

where d is the print diagonal, proportional to h for the indenter used in this study. The linear term, $b_2 d$, expresses the hardness dependence to the indentation depth (size effects).

Original statistical treatment

As previously mentioned, the first contact definition is a complex issue in indentation tests. As the actual position of the first contact remains uncertain, we proposed a method based on the definition of a relative referential. Instead of searching the true first contact position, the curves are localised by the difference between their shape described by Bernhardt's model and the position predicted by this model.

Hardness H is usually defined as:

$$H = P/A_c, \tag{7}$$

where A_c is the contact area. With a Berkovich indenter, the contact area A_c can be expressed using the contact depth h_c: $A_c = 24.56 {h_c}^2$. Thus, the previous equation becomes:

$$P = \alpha H h_c^2 \qquad \text{with} \qquad \alpha = 24.56. \tag{8}$$

The introduction of a deviation, Δh_c, modifies Equation 8 as follows:

$$P = \alpha H (h_c + \Delta h_c)^2 \tag{9}$$

Then, we take into account the possibility of an ISE through the use of Vingsbo's law [21] defined as $H = H_0 + \beta/h_c$, where H_0 is the macroscopic hardness and β is the ISE factor. It is worth noting that the linear relationship between the load and the penetration depth at the early stage of the indentation test gathers different phenomena known as the ISEs. Such linear relationship yields to a proportionality between H and ${h_c}^{-1}$, through a constant term, β, named ISE factor.

Thus, the previous equation is modified as follows:

$$P = \alpha\left\{H_0 h_c^2 + [2\Delta h_c H_0 + \beta] h_c + 2\beta\Delta h_c + H_0 \Delta h_c^2 + \Delta h_c^2 \beta / h_c\right\}. \tag{10}$$

When h_c is high compared with Δh_c, the previous equation becomes:

$$P \approx \alpha\left\{H_0 h_c^2 + \left[2\Delta h_c H_0 + \beta\right] h_c\right\} = \alpha.\left\{c_1 h_c^2 + c_2 h_c\right\}. \tag{11}$$

The obtained formula is similar to Equations 5 and 6. It is important to note that the linear term h_c is multiplied by the sum of two terms: $2\Delta h_c H_0$ and β. If the error on the zero point is small, the term β can be easily identified. On the other hand, if the ISE factor, β, is of the same order of magnitude than the term $2\Delta h_c H_0$ then, the identification of ISE is difficult. This possibility will be further studied in the section dedicated to the results and discussion.

To dissociate the size effects from errors caused by first contact detection, we simultaneously treat all the indentation curves. Thus, the macrohardness and ISE factor are determined through a mathematical optimisation that considers all the experimental curves as a whole.

For the optimisation, we assume that each curve can be described by Equation 10 that the hardness and the ISE factor are homogeneous on the whole specimen. It means that H_0 and β remain constant whatever the selected curve [22]. By contrast, the deviation value Δh_{ci} is different for each curve i, as it defines the gap between the experimental data and the evolution predicted by conventional hardness equation. The optimisation procedure aims to determine the macrohardness H_0, the size effect factor β and the gap vector $\mathbf{\Delta}$, whose components correspond to the deviation Δh_i of each curve i. This calculation is made through the use of a quadratic optimisation method that leads to minimise the following function:

$$\min_{H_0, \Delta_1 \cdots \Delta_n, \beta} \sum_{i=1}^{n} \sum_{j=1}^{p_i} \left[P_{i,j} - \alpha\Big(H_0 . h_{cj}^2 + (2.\Delta h_{ci} . H_0 + \beta) h_{cj} + 2.\beta.\Delta h_{ci} + H_0 . \Delta h_{ci}^2 + (\Delta h_{ci}^2 . \beta)/h_{cj} \Big) \right]^2, \tag{12}$$

where index i refers to curve i while index j corresponds to the j-th couple (P, h) of the load versus indentation depth curve.

The proposed method is applied to the experimental indentation data given by the four specimens having different roughness.

Results and Discussion

Efficiency of the proposed method

To be able to guarantee the size effect presence, it is important to determine the value of Δh_c and β with their respective confidence intervals. It is realised through the use of a double Bootstrap (recent resampling technique) on the one hundred experimental curves. The first Bootstrap enables the simulation of noise in a given loading curve. The second Bootstrap permits to practise a simple random sampling with replacement. This sampling method is repeated 1000 times to reproduce the specimen heterogeneity. The average values and standard deviations are calculated for H_0, β and Δh_c.

Figure 4 depicts the average and standard values calculated for the macrohardness H_0 through the minimisation, using a double Bootstrap. The average values globally decrease with an increase in the polishing paper number. This evolution was expected as high paper grit numbers are made of fine abrasive particles which entail a lower hardening of the surface than coarse abrasive particles in the same polishing conditions. The standard deviation values are globally low as they are inferior to 0.007 GPa. This result shows the method robustness for the quantification of the macrohardness.

On Figure 5, a histogram represents the ISE factor distributions calculated for each specimen, using a double

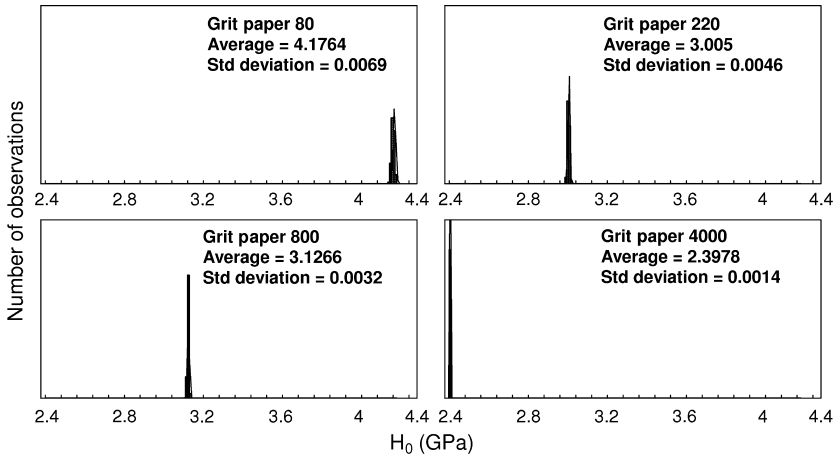

Figure 4: Histogram of the macrohardness (H_0) values calculated through the use of a double Bootstrap

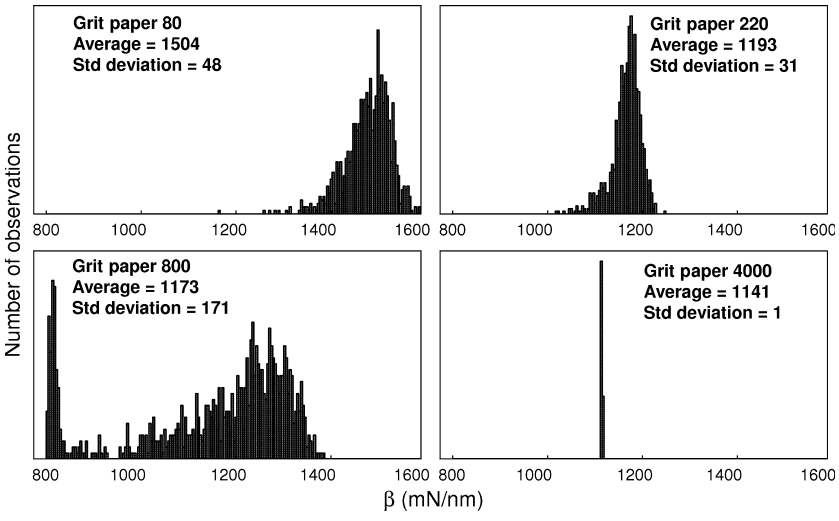

Figure 5: Histogram of the ISE factor (β) values calculated through the use of a double Bootstrap

Bootstrap. The average values of the ISE factor lie between 1100 and 1500 mN/nm. The ISE factor values tend to decrease with the increase in the paper grit numbers. A relatively high standard deviation is observed for the specimens having a rough surface: 48 and 31 mN/nm for specimens polished with grit paper 80 and 220, respectively. The results obtained with the specimen polished with grit paper 800 departs from the previous observations as it has a standard deviation equal to 171 mN/nm, thus five times more important. This difference has not been explained yet.

Figure 6 depicts the distribution calculated for the deviations (Δh_c) between the shape of the experimental curves and the evolution predicted by Equation 8. A decrease in the scatter is observed with a finer polishing. This scatter is characterised by standard deviations varying from 15.4 to 100 nm for the specimens polished with grit paper 4000 and 80, respectively. As expected, roughness significantly affects the first contact detection and increase the scattering between the experimental curves.

Simultaneous treatment of the curves and ISE evaluation

According to Equation 11, if the term $2\Delta h_c H_0$ has a same order of magnitude as the ISE factor β (Equation 11), then the ISE identification could be influenced by the deviation Δh_c. A global appreciation of the average and standard deviation values calculated for H_0, β and Δh_c shows that, for extreme values, the deviations for the zero-point localisation can seriously affect the ISE evaluation. Hence, the size effects cannot be distinguished from the deviation by only taking into account a single load versus indentation depth curve. A similar issue is encountered with the non-instrumented microindentation. Schneider *et al.* [14] showed that a high number of measurements at a given load was necessary to detect size effects. This number increase is inversely proportional to the indentation depth.

Currently, the identification of these effects is based on the use of a single curve [23] or on a set of curves that is statistically poor (typically a dozen of curves). The evaluation of the ISE requires a statistical treatment performed on a representative sample. The simultaneous treatment proposed here enables to evaluate the ISE and thus to accurately determine the macrohardness.

Effect of roughness

As the deviation values are significantly different in each abraded specimen, an attempt to quantify the influence of roughness on the nanoindentation tests is performed. Such

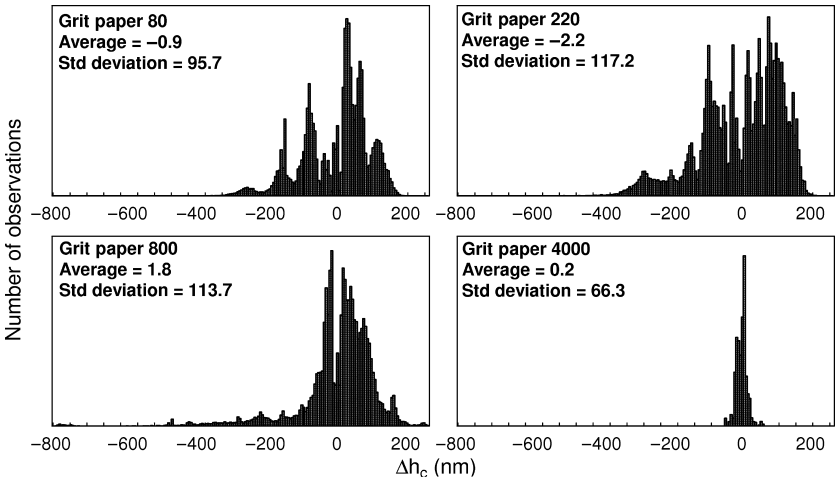

Figure 6: Histogram of the values of the gaps between the experimental loading curves and the curves predicted by Kick's law, calculated with a double Bootstrap

a study is difficult to handle with because it implies the use of roughness parameters whose values are intimately linked with the evaluation length chosen for their calculation (see Figure 3). The arbitrary choice for the evaluation length risks biasing the roughness parameter values and thus may introduce errors in the analysis results. To deal with this issue, a statistical study is developed.

The different scatters obtained for the nanoindentation curves (Figure 2) may be an evidence of an interaction between the indentation results and the surface preparation quality. Rougher surfaces seem to give greater values for the deviations between the experimental curves and the evolution predicted by Equation 8. Two indicators are built to try to quantify the observed scatter: the RMS roughness and the standard deviation of the gaps. As mentioned when dealing with the 'Multiscale pre-treatment of two-dimensional experimental profiles', the RMS roughness value depends on the considered scale. The difficulty is thus to determine the relevant scale for roughness measurement, *that is,* the scale at which the measured roughness influences the gap values. In fact, nanometric roughness will be important for small scales while it will not be perceived at a large scale of evaluation. To find the evaluation length, we search the best correlation between the standard deviation values of the gaps obtained for the different abraded specimens and the four RMS roughness values calculated using different evaluation lengths.

Figure 7 illustrates the results obtained for the evaluation lengths equal to: 3.8, 12.9, 377 and 3773 μm. The best correlation between the RMS roughness and the gaps is obtained for evaluation length values comprised between 3 and 13 μm. A *quasi* linear relationship is obtained with a coefficient of determination approximately equal to 0.9. The correlation only takes place from 3 μm because for smaller values the rugosimeter tip has a filtering effect towards roughness. For values higher than 13 μm, low

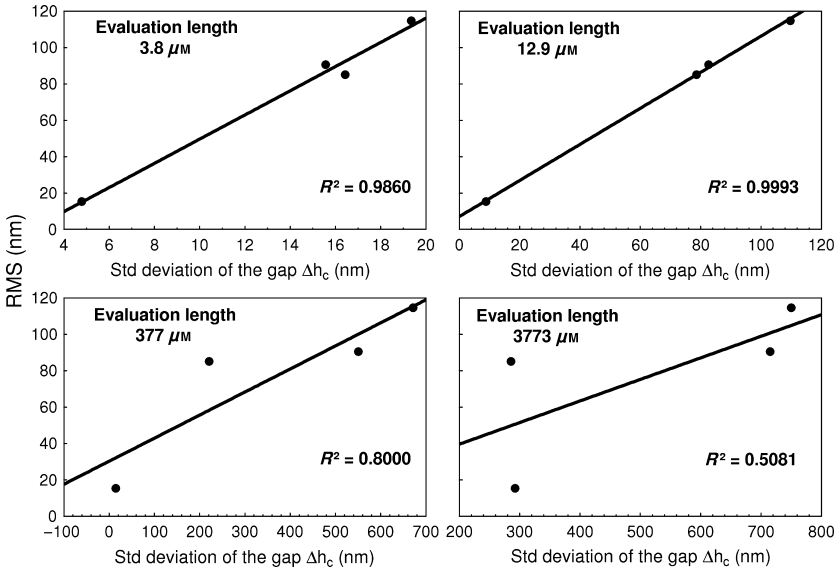

Figure 7: Evolution of the root-mean-square roughness (RMS) versus the standard deviation values of the gaps between the shapes experimental loading curves and the shapes predicted by Kick's law, for evaluation lengths equal to 3.8, 12.9, 377 and 3773 μm

frequency components are introduced in the signal and disturb the correlation between the roughness and the gaps. The correlation between both parameters means that the surface topographical variations are approximately equal to the deviations of the experimental data from conventional hardness description. It shows the effectiveness of the zero-point correction. These results also underline the need for a careful surface preparation of the specimens for the nanoindentation tests to avoid any disturbance of the results.

Conclusion

An original treatment method is proposed to accurately determine by nanoindentation the macrohardness and to evaluate the ISE. The data treatment aims at compensating the errors created by the inaccurate zero-point determination, which leads to large scattering of the experimental indentation curves. The method is successfully applied to specimens having rough surface (average roughness equal to 1140 nm) to mirror-like surfaces (average roughness equal to 20 nm).

The standard deviation for the estimated macrohardness is small which indicates the robustness of the proposed approach.

The building of the method equations enabled to emphasise the fact that the ISEs cannot be accurately evaluated using a single indentation curve. In such situation, error in macrohardness estimation can significantly increase because of a bad consideration of the ISE. To prevent this misinterpretation, the curves should be treated simultaneously instead of averaging results of separately treated curves.

A clear correlation is observed between the RMS roughness and the standard deviation values of zero-point corrections, which highlights the effect of surface topography on the scattering of the indentation curves. Hence, specimens used for nanoindentation test should be polished carefully.

This work will be further extended using specimens showing other magnitudes of surface roughness and materials showing different ISEs sources (e.g. pile-up, sink-in, surface oxide layer…).

REFERENCES

1. Cole, D. P., Bruck, H. A. and Roytburd, A. L. (2009) Nanomechanical characterisation of graded NiTi films fabricated through diffusion modification. *Strain* **45**, 232–237.
2. Ou, K. S., Yan, H. Y. and Chen, K. S. (2008) Mechanical characterization of KMPR by nano-indentation for MEMS applications. *Strain* **44**, 267–271.
3. Shuman, D. J., Costa, A. L. M. and Andrade, M. S. (2007) Calculating the elastic modulus from nanoindentation and microindentation reload curves. *Mater. Charact.* **58**, 380–389.
4. Kim, J.-Y., Kang, S.-K., Greer, J. R. and Kwon, D. (2008) Evaluating plastic flow properties by characterizing indentation size effect using a sharp indenter. *Acta Mater.* **56**, 3338–3343.
5. Jäger, A. and Lackner, R. (2009) Finer-scale extraction of viscoelastic properties from nanoindentation characterised by viscoelastic–plastic response. *Strain* **45**, 45–54.
6. Grau, P., Berg, G., Fränzel, W. and Meinhard, H. (1994) Recording hardness testing. Problems of measurement at small indentation depths. *Phys. Stat. Solid (A)* **146**, 537–548.
7. Fischer-Cripps, A. C. (2006) Critical review of analysis and interpretation of nanoindentation test data. *Surf. Coat. Technol.* **200**, 4153–4165.
8. Chudoba, T., Schwarzer, N. and Richter, F. (2000) Determination of elastic properties of thin films by indentation measurements with a spherical indenter. *Surf. Coat. Technol.* **127**, 9–17.
9. Ullner, C. (2000) Requirement of a robust method for the precise determination of the contact point in the depth sensing hardness test. *Measurement* **27**, 43–51.
10. Kalidindi, S. R. and Pathak, S. (2008) Determination of the effective zero-point and the extraction of spherical nanoindentation stress-strain curves. *Acta Mater.* **56**, 3523–3532.
11. Oliver, W. C. and Pharr, G. M. (1992) An improved technique for determining hardness and elastic modulus using load and displacement sensing indentation experiments. *J. Mater. Res.* **7**, 1564–1583.
12. Bigerelle, M., Van Gorp, A. and Iost, A. (2008) Multiscale roughness analysis in injection-molding process. *Polym. Eng. Sci.* **48**, 1725–1736.
13. ENISO-4287 (1997) Geometrical Product Specifications (GPS). Surface texture: profile method. terms, definitions and surface texture parameters, Geneva, Switzerland.
14. Schneider, J. M., Bigerelle, M. and Iost, A. (1999) Statistical analysis of the vickers hardness. *Mater. Sci. Eng., A* **262**, 256–263.
15. Bigerelle, M., Giljean, S. and Mathia, T. G. (2011) Multiscale characteristic lengths of abraded surfaces: three stages of the grit-size effect. *Tribol. Int.* **44**, 63–80.
16. Bigerelle, M., Mathia, T. and Bouvier, S. (2012) The multi-scale roughness analyses and modeling of abrasion with the grit size effect on ground surfaces. *Wear* **286–287**, 124–135.
17. Kick, F. (1885) Das Gesetz der proportionalen Widerstände und seine Anwendungen : nebst Versuchen über das Verhalten verschiedener Materialien bei gleichen Formänderungen sowohl unter der Presse als dem Schlagwerk Verlag von Arthur Felix.
18. Tabor, D. (1951) *The Hardness of Metals*. Clarendon Press, Oxford.
19. Bernhardt, E. O. (1941) On microhardness of solids at the limit of Kick's similarity law. *Z. Metallkd.* **33**, 135–144.
20. Li, H. and Bradt, R. C. (1993) The microhardness indentation load/size effect in rutile and cassiterite single crystals. *J. Mater. Sci.* **28**, 917–926.
21. Vingsbo, O., Hogmark, S., Jönsson, B. and Ingemarsson, A. (1986) *Indentation Hardness of Surface-Coated Materials*, ASTM STP edn. ASTM STP, Philadelphia, USA.
22. Bigerelle, M., Mazeran, P. E. and Rachik, M. (2007) The first indenter-sample contact and the indentation size effect in nano-hardness measurement. *Mater. Sci. Eng., C* **27**, 1448–1451.
23. Kim, J.-Y., Kang, S.-K., Lee, J.-J., Jang, J.-i., Lee, Y.-H. and Kwon, D. (2007) Influence of surface-roughness on indentation size effect. *Acta Mater.* **55**, 3555–3562.